ACS APPLIED NANO MATERIALS
Cite This: ACS Appl. Nano Mater. 2018, 1, 564−571
Article
www.acsanm.org

Proton Conducting Polyoxometalate/Polypyrrole Films and Their Humidity Sensing Performance

Jun Miao,[†,‡] Yulong Chen,[†,‡] Yiwen Li,[†,§] Jiaji Cheng,[∥] Qingyin Wu,[⊥] Kar Wei Ng,[†] Xin Cheng,[‡] Rui Chen,[§] Chun Cheng,*[,‡] and Zikang Tang*[,†]

[†]Institute of Applied Physics and Materials Engineering, University of Macau, Avenida da Universidade, Taipa, Macau, P. R. China
[‡]Department of Materials Science and Engineering, Southern University of Science and Technology, Shenzhen, Guangdong 518055, P. R. China
[§]Department of Electrical and Electronic Engineering, Southern University of Science and Technology, Shenzhen, Guangdong 518055, P. R. China
[∥]Chimie et Biologie des Membranes et des Nanoobjets (CBMN), CNRS—Université Bordeaux—Bordeaux INP, UMR 5248, Allée St Hilaire, Bat B14, 33607 Pessac, France
[⊥]Department of Chemistry, Zhejiang University, Hangzhou, Zhejiang 310027, P. R. China

Supporting Information

ABSTRACT: Proton conducting polyoxometalate has received considerable attention because of its unique structural properties. This article reports the fabrication of hybrid polymer films of polypyrrole/polyoxometalate and their resistive-type humidity sensing performance. Hybrid polymer films with different thicknesses were prepared via the coelectrodeposition of free pyrrole monomers with metal oxide clusters. A sensing response of 1.9 s and a recovery time of 1.1 s were exhibited in a 59 nm thick sample at 98% relative humidity and in a sensing range of 11−98% relative humidity. The outstanding sensing in the polypyrrole chain could be ascribed to the synergistic effect of the proton acid doping structure and the oxidation doping structure. The humidity sensor based on the nanocomposite was repeatable even after two months with good response and recovery times.

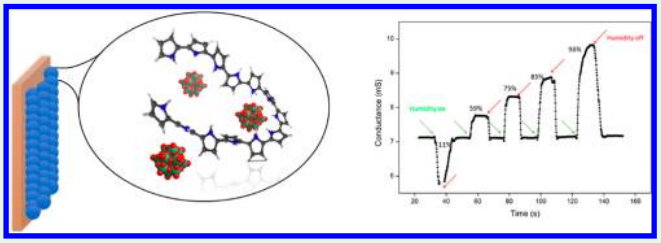

KEYWORDS: *proton conduction, polyoxometalate, conductive polymer, humidity sensor*

INTRODUCTION

To date, one of the key topics in current science and technology is sensing.[1,2] Sensing humidity is important in many areas including environmental control, industrial processing, human health, clinical diagnosis, the automobile industry, and agriculture.[3−7]

Conductive polymers have attracted extensive theoretical interest and practical applications in sensing technology.[4,6,8] These polymers could be utilized for various purposes and may offer distinct possibilities.[9−12] Because of its excellent electrical and mechanical properties and thermal durability, polypyrrole (Ppy) is a promising candidate for sensor applications.[13−20] In contrast, their inevitable drawbacks are poor linearity and a relatively long response time, which is typically several tens of seconds or even minutes. Recently, many conducting polymers, such as zinc oxide/polypyrrole,[18] a nanocrystalline-based polyimide film[21] and a redox conducting supramolecular ionic material,[22] exhibited both high sensitivity and a fast response time compared with those shown by the pure components by taking full advantage of the high hygroscopicity and water stability arising from one material and the hydrophobic interactions from the other material.

Similar to polymeric materials, nanoscale metal oxides have been widely utilized for the fabrication of humidity sensing materials because of their superior thermal durability, their moisture-resistance to avoid degradation, and a broad range of operating environments.[23−30] Polyoxometalates (POMs), a class of early transition metal oxide clusters, are considered one potential research area in sensing materials.[31−37] POMs are defined as a class of metal oxide clusters that are entirely distinguishable from most metal oxides, revealing a large variety of molecular structures from the nanoscale to the microscale.[38,39] In this context, one of the most significant properties of POMs is the ability to accept and release a specific number of electrons without a decomposition or a change in their original structures.[40] The types of interactions between the organic cationic components and inorganic anionic components play a vital role in the properties exhibited by the hybrid ionic materials.

In this paper, for the first time, we report the design and synthesis of humidity sensing films based on a POM/Ppy

Received: October 24, 2017
Accepted: January 5, 2018
Published: January 5, 2018

DOI: 10.1021/acsanm.7b00072
ACS Appl. Nano Mater. 2018, 1, 564−571

nanocomposite, as shown in Figure 1a. For the preparation of a humidity sensing material, the polyoxoanion of POM, a

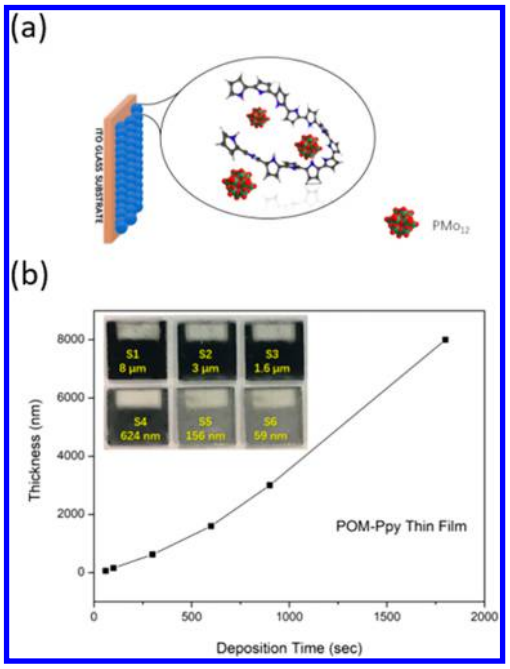

Figure 1. (a) Schematic illustration of the synthetic process of the POM/Ppy thin film: synthesis of PMo_{12}–Ppy via a green electrodeposition reaction. (b) Deposition time vs film thickness of the POM/Ppy thin film. Inset: photograph of the POM/Ppy thin film with electrodeposition time.

reversible and fast redox electrolyte used in electrochemical deposition reactions, was chosen as the anionic building block, and protonated polypyrrole was selected as the cationic building block because of its relatively large size and hydrophobicity. The responses of the sensing films with various thicknesses were measured at five different humidity levels from 11% to 98% relative humidity (RH). The optimal sample was further tested for durability, repeatability, hysteresis, and response/recovery time. Compared with a POM-based ionic crystal,[41,42] POM/conductive polymer (CP) nanocomposites exhibit an advantage during the formation of uniform films. Compared with the POM–polyethylene glycol (PEG) composites,[43] the POM/Ppy-based humidity sensor exhibits high sensitivity. The judicious choice of POM/CP nanocomposites for humidity sensing films will permit high sensitivity and fast response. This work will provide a new method for the design and synthesis of practical humidity sensing materials.

EXPERIMENTAL SECTION

Preparation of the POM/Ppy Film. Coelectrodeposition was carried out using a chronoamperometric technique on a Zennium X workstation. A chronoamperometric potential (+0.75 V) was applied continuously for a specific period of time to obtain the POM/Ppy film. The electrolyte solution for POM/Ppy electroplating was prepared by mixing a 7 mM pyrrole monomer (98%, Sigma-Aldrich) and 5 mM POM ($H_3PMo_{12}O_{40}{\cdot}xH_2O$) in deionized (DI) water for 0.5 h. The pH of the final solution is ~2.8 to prevent $[PMo_{12}O_{40}]^{3-}$ from decomposition. Finally, the POM/Ppy films after electrodeposition of POM/Ppy were carefully removed from the bath and cleaned repeatedly with DI water and ethanol. Different ratios of POM and Ppy (7 and 2.5 mM, and 7 and 10 mM, respectively) were used as the reference sample.

Morphological and Structural Characterization. The microstructure and morphology of the POM/Ppy film were investigated using scanning electron microscopy (SEM, Zeiss Sigma FESEM and TESCAN VEGA 3 LMH). The transmission electron microscopy (TEM) images were obtained using an FEI Tecnai F30 microscope. The chemical composition was evaluated using Raman spectroscopy (HORIBA LabRAM HR Evolution) equipped with laser excitation (532 nm). Thickness measurements were conducted using a Stylus Profiler (KLA-Tencor D-120) instrument.

Humidity Sensor Measurements. The humidity test setup consisted of a sealed Makrolon chamber in which to place the samples, a Keithley 4200A-SCS parameter analyzer, a gas pump, and a compressed air source. Two copper wires were connected to the two silver paste electrodes to make electrical contacts. By using K_2SO_4, KCl, NaCl, NaBr, and LiCl saturated solutions, the different humidity environments were obtained which correspond to approximately 98%, 85%, 75%, 59%, and 11% RH, respectively. By probing the fluctuation in the dc conductance of POM/Ppy, the response of the humidity sensors was measured. The sensitivity is denoted as S ($S = \Delta C/C_{air}$), where ΔC and C_{air} denote the conductance change in humid environments and the conductance in air, respectively. The response time ($\xi_{response}$) is defined as the period required for a 90% increment in conductance after the humid air was switched on. Similarly, the recovery time ($\xi_{recovery}$) is the period required for a 90% reduction in conductance after the humidity was switched off. The environmental humidity was approximately 46%, and the temperature was 25 °C.

RESULTS AND DISCUSSION

POM/Ppy thin films have been plated onto indium tin oxide (ITO) glass substrates by using an electrodeposition method. The process is based on the cation-radical electropolymerization processes of pyrrole with the participation of solution anions.[44] In electrochemical polymerization, the pyrrole monomer first competes with the anion in the electrolyte to adsorb onto the electrode; Py is oxidized into the cation ($Py^{\bullet+}$) and forms a neutral ionic pair ($Py_3^{+}A^{3-}$) with the anion (A^{3-}) simultaneously. Then, the ion pair is deprotonated to form a pyrrole trimmer, which is oxidized as a cationic radical and combined with the anion to form an ionic pair. The cationic radicals are then coupled to each other to cause the growth in the polypyrrole chain. For an investigation of the thin film thickness dependence on the electrochemical properties, six different samples were prepared with electrodeposition times of 1800, 900, 600, 300, 100, and 60 s. The thicknesses of the six samples, which were measured using a Stylus Profiler (KLA-Tencor D-120) instrument, were 8 μm, 3 μm, 1.6 μm, 624 nm, 156 nm, and 59 nm, as shown in Table S1 in the Supporting Information. Figure 1b demonstrates a plot of film thickness versus deposition time, which shows that the film growth is approximately linear with time. It is noted that there is a more rapid growth in film thickness with longer deposition times.

The Raman spectrum obtained with an incident laser beam at 532 nm is demonstrated in Figure S1 in the Supporting Information and is representative of the POM/Ppy films. The peaks at 1601 and 1429 cm^{-1} were assigned to C=C and C—C stretching vibrations, respectively.[45] The C—N stretching vibrations led to the peaks at 1338 cm^{-1}.[46] The intensity ratio of the C=C and C—C stretching bands for the POM/Ppy films (2.55) was greater than that of the Ppy films (2.36), indicating the increased conjugation length of the Ppy chains in POM/Ppy.[19] The spectrum of the POM/Ppy film shows a relatively strong band at 1004 cm^{-1}. This band was assigned to the characteristic symmetric stretch of the Mo—O_t bonds ($\nu 1$) in $[PMo_{12}O_{40}]^{3-}$, which is comparable to the characteristic band observed at 1016 cm^{-1} for $H_3PMo_{12}O_{40}{\cdot}14H_2O$.[47]

DOI: 10.1021/acsanm.7b00072
ACS Appl. Nano Mater. 2018, 1, 564–571

Scanning electronic microscopy (SEM) photographs demonstrate that the diameters of the grains in the polypyrrole and POM/Ppy films are approximately 20−200 nm, and the electrodeposited POM/Ppy film on an ITO glassy electrode have a rather smooth structure owing to the agglomeration of particles with sizes of tens of nanometers or smaller, which are different from the PPy films prepared by spin coating, as shown in Figure 2a and Figure S2 in the Supporting Information. A

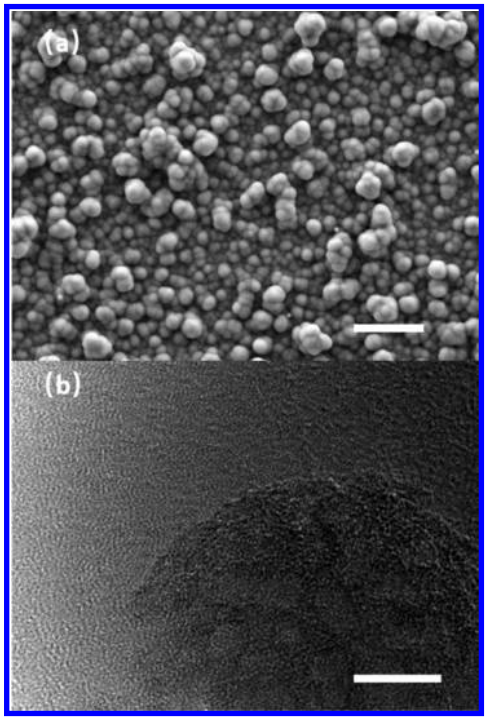

Figure 2. (a) SEM of the POM/Ppy film grown electrochemically onto the ITO glassy electrode (scale bar, 200 nm). (b) HRTEM images of the POM/Ppy film (scale bar, 5 nm).

probable reason for this is that the reaction mechanism of the coelectrodeposition between POM and pyrrole is a cation-radical electropolymerization process involving the participation of solution anions.[44,48] The polymerization of pyrrole and the deposition of POM are competitive reactions during the formation process of the POM/Ppy films. The nanostructures help to enhance the humidity sensitivity of the film, which can result in the high conductance and the sensitivity of the copolymer films to humidity as well as its excellent attachment to the substrate. HRTEM images have been taken to clearly observe the growth in the composite film, as shown in Figure 2b. However, no obvious lattice fringes were observed, indicating the existence of a PMo_{12} cluster as an anion (a dispersive cluster, not a crystal particle). Energy-dispersive spectrometer (EDS) was used to examine the composition of the POM/Ppy. As shown in Figure 3, five elements, C, N, O, P, and Mo, are identified in this spectrum. This result indicates that the PMo_{12} clusters (ca. 1.0 nm) are homogeneously dispersed in the ionic network. It is demonstrated that both the polymerization of pyrrole and the deposition of POM are competitive reactions during the formation of the POM/Ppy films. The composition of the reference samples was also examined by using EDS. There is no obvious difference between the reference samples (Figure S3 in the Supporting

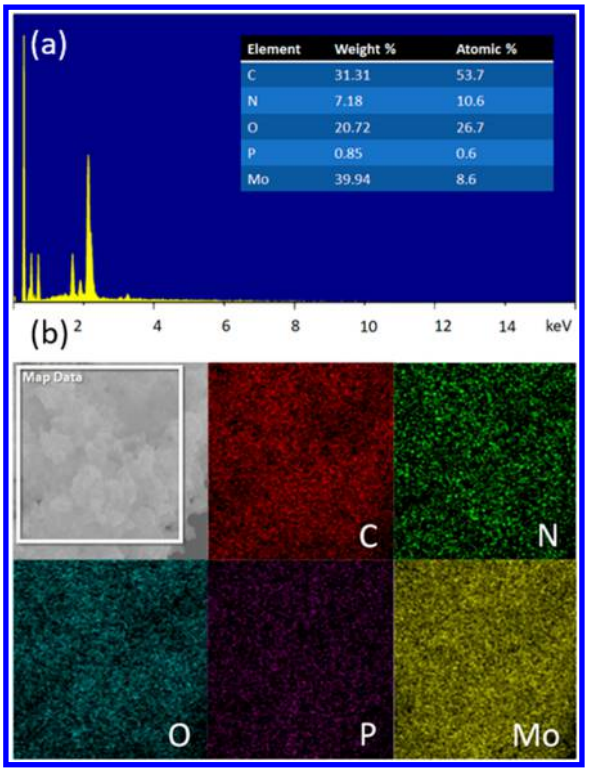

Figure 3. (a) Energy-dispersive spectrometry (EDS) pattern of the POM/Ppy film. (b) EDS elemental mapping analysis of the POM/Ppy film.

Information), which can be ascribed to the cation-radical electropolymerization processes with the anions in the solution.

The chemoresistive sensor device, as demonstrated in Figure 4a, was first made accessible to pressurized air for approximately 30 min to obtain a static baseline conductance, and the conductance of the sample changes with a fluctuation in the humidity. The humidity sensing performance at room temperature was measured in ambient humidity with 46% RH. The response and recovery curve of the POM/Ppy humidity

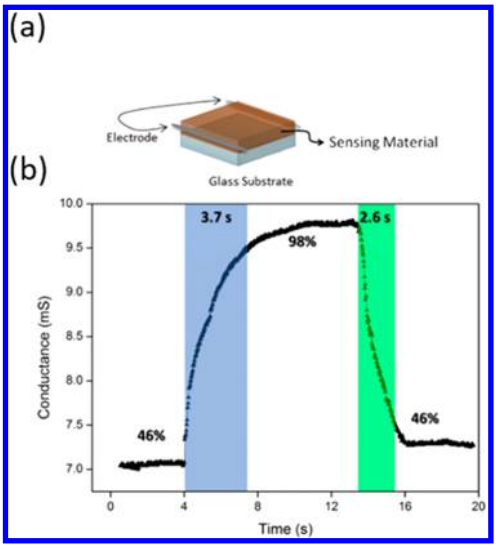

Figure 4. (a) Schematic representation of the humidity sensors. (b) Response and recovery of a typical humidity sensor based on POM/Ppy-S4 at 25 °C.

DOI: 10.1021/acsanm.7b00072
ACS Appl. Nano Mater. 2018, 1, 564−571

sensor at 98% RH is demonstrated in Figure 4b. It was observed that the conductance of the sensor increases gradually with increasing humidity. The conductance increase can be explained as a combination of the following two processes: (i) The absorption of water molecules on the metal oxide cluster surface has been shown to be a dissociative mechanism to form hydroxyl groups. The water molecules adsorbed on the grain surface react reversibly with molybdenum oxide clusters. (ii) The terminal oxygen of metal oxide cluster reacts with H^+ coming from the dissociation of water vapor to form hydroxyl groups (heteropolybules). Because of the free electrons given by this reaction, the conductance increases with increase in humidity. The sensitivity of the sensor based on the POM/Ppy film was 758 μS/% RH at 98% RH, which is higher than that of the other types of Ppy humidity sensors.[14,18,45] The surface oxygen atoms of the POMs provided the larger number of active sites, which was attributed to the improved sensitivity. Moreover, the POM/Ppy sensor showed more rapid response and recovery times of 3.7 and 2.6 s, respectively, as shown in Figure 4b. For a further investigation of the humidity sensing performance of the POM/Ppy sensor, the dynamic response was measured at the room temperature. Figure 5a demonstrates

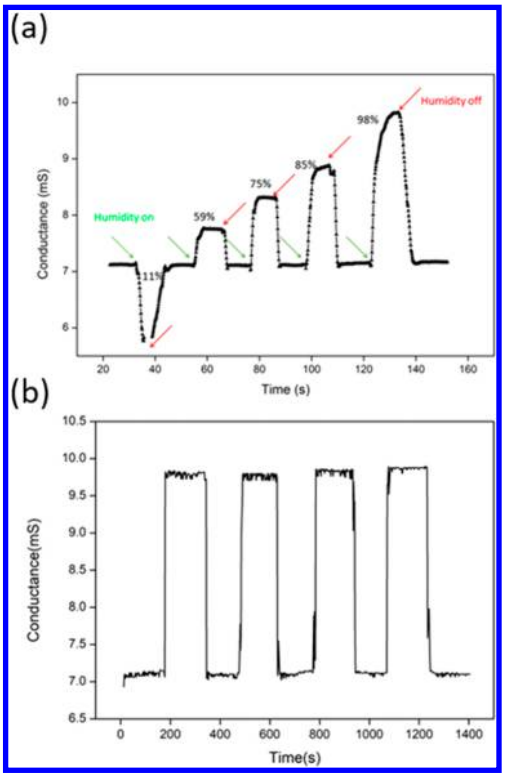

Figure 5. (a) Typical response curves of the POM/Ppy-S4 sensor to various RH values at 25 °C. (b) Dynamic response curve to 98% RH at 25 °C.

the typical response properties of the RH values differing from 11% to 98% RH. The resistance increased with the humidity of 11% because of desorption of water on polypyrrole with decrease in humidity. The conductance signal fluctuates rapidly with different RH values. Figure 5b demonstrates the dynamic properties at 98% RH for four cycles. There is only a negligible change in sensitivity, indicating the durability of the sensor operating at room temperature.

The typical response curves reveal obvious changes in the humidity-response behavior of the POM/Ppy nanocomposites in comparison with those of the other Ppy samples.[14,18,20,30] The presence of POM plays a vital role in the increase in conductance. This increase may be due to the porous morphology of the polypyrrole, as demonstrated in the SEM and TEM photographs. Initially, the water molecules exposed to the POM/Ppy nanocomposites facilitate a possible swelling of the framework, and more proton transfer pathways are constructed.[43,49] As a result of the swelling nanocomposite, the polymer chains and the metal oxide clusters are tensioned together producing a better connectivity of the network. The degree of swelling depends on the bonding between the polypyrrole chains and POMs, the stability of the exposure of the POM/Ppy nanocomposite to the surrounding environment, and its physical and chemical nature. This phenomenon consequently induces an increase in the conductance value, as demonstrated in Figure 5. The conductance C is established in the following equation:[50]

$$C_0/C = (s/s_0)\exp[\gamma \Delta s]$$

where C_0 is the initial conductance before swelling, Δs is the change in separation (between the metal oxide particles and the conductive polymer) under swelling, and γ is a factor that depends on the potential barrier height between the metal oxide particles and the conductive polymer.

To show the hysteresis of the sensor, the equilibrium conductance of the device was measured at various humidity levels with increasing humidity from 11% to 98% RH and then decreasing back to 11% RH again. Figure 6 shows the

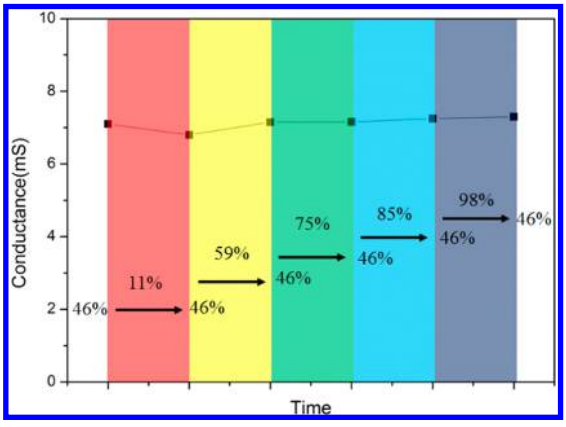

Figure 6. Equilibrium conductance of the POM/Ppy humidity sensor when it was exposed to air after testing under different relative humidity conditions.

equilibrium conductance of the humidity sensor in ambient environment after measuring at various RH levels. The equilibrium conductance scarcely increased when the sensor was removed from the higher humidity level to ambient environment and scarcely decreased when it was removed from the lower humidity level to ambient humidity, demonstrating a very slight hysteresis when operating at room temperature.

The response/recovery times were investigated to compare the sensing properties of the POM/Ppy films with various thicknesses while working at room temperature, as shown in Figure 7. The sensors with thicknesses ranging from 8 μm to 59 nm showed fast response and rapid recovery times from 9.8 s/8.7 s to 1.9 s/1.1 s, respectively, at 98% RH. This ultrafast

DOI: 10.1021/acsanm.7b00072
ACS Appl. Nano Mater. 2018, 1, 564−571

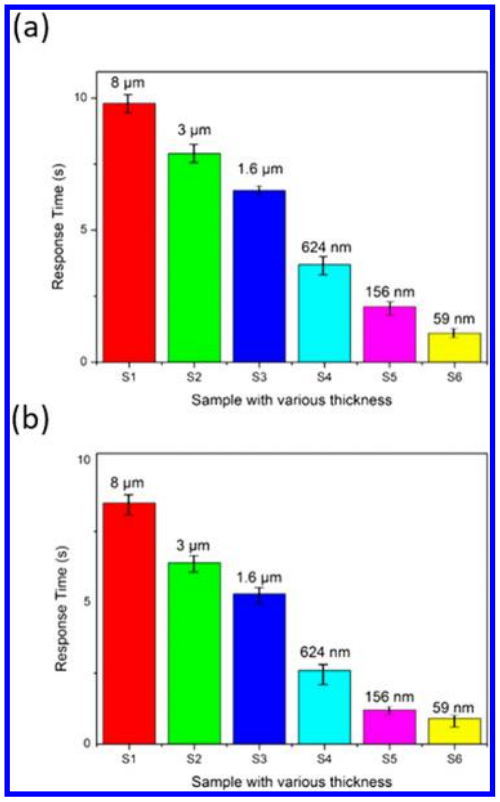

Figure 7. (a) Response times and (b) recovery times of the POM/Ppy sensor with various thicknesses under 98% RH at room temperature.

response behavior can be explained by the polarizability and transferability of the polyoxoanions.[51] However, the sensitivities of S5 and S6 exhibit an obvious change, and the linearity of the typical curve ceases to be a first-order linear relationship. However, the response and recovery times of the sample are the shortest among the 6 samples (see Figures S9 and S10 in the Supporting Information), which may result from the limited water absorption capacity of the thinner films.

It has been demonstrated in Figure 5 that the conductance of the POM/Ppy samples increased with increasing humidity. Two conduction mechanisms proceed simultaneously: One is electron conduction through the Ppy chains with H_2O as electron donors, and the other is proton conduction through the terminal oxygen atoms of the POMs, the main chain of the polypyrrole, and the continuous H_2O chains by the Grotthuss mechanism, as shown in Figure 8. The results indicate the following: (i) Water vapor is adsorbed onto the POM surface and reacts reversibly with the molybdenum oxide clusters. The terminal oxygen of the metal oxide cluster reacts with H^+ resulting from water vapor dissociation to form hydroxyl groups (known as heteropolybules). (ii) It has been reported that the charge transfer between POM and H_2O enhances the proton conductivity of the POM-based material in the presence of humidity.[52−56] In this case, besides p-doping, the β-C of the pyrrole units was protonated with a positive charge transfer to the main chain of the polypyrrole. The H_2O adsorbs onto the sensing material and serves as proton hopping sites. Thus, the proton conductivity of the POM-based material increases in the presence of humidity.

The POM/Ppy films show characteristics of a temperature-dependent electron conductivity in accordance with the Mott variable-range hopping model:

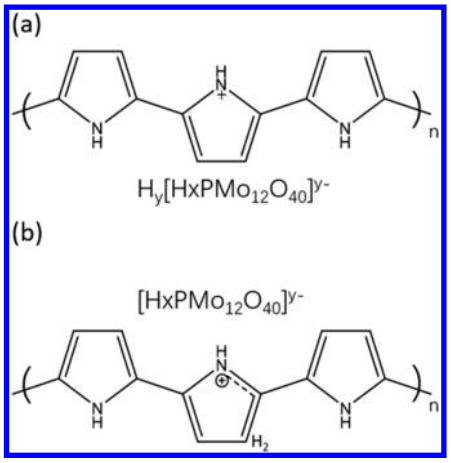

Figure 8. Two doping structures of conducting polypyrrole. (a) Counteranion doping structure with the oxidation of the conjugated chain. (b) Proton acid doping structure.

$$\delta(T) = \delta_0 \exp[-(T_0/T)^{1/(n+1)}]$$

where n is the dimension of the space, and when n = 1, 2, and 3, it represents one-, two-, and three-dimensional variable-range hopping conduction.[57] The temperature dependence of the conductivity was studied in the temperature range 25−85 °C. Both Ppy and POM/Ppy conform to an approximately linear relation between the log δ and $T^{-1/4}$ (as shown in Figure 9), indicating the Mott variable-range hopping mechanism in three dimensions.

Furthermore, for an investigation of the humidity properties of the POM/Ppy sensor at elevated temperatures, the dynamic

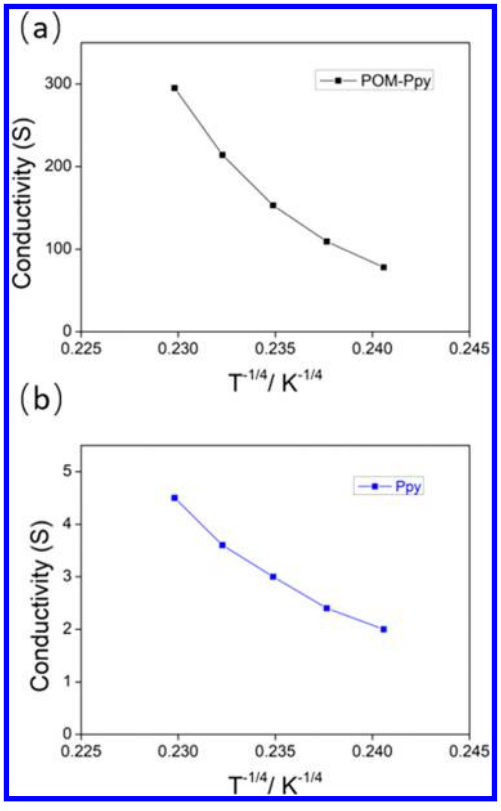

Figure 9. Mott plots of the conductivity of (a) POM/Ppy and (b) Ppy.

DOI: 10.1021/acsanm.7b00072
ACS Appl. Nano Mater. 2018, 1, 564−571

Table 1. Comparison of the Sensors Based on Polypyrrole and/or Its Composites with Other Inorganic Materials

sensor type	sensing material	measurement range	response/recovery time	ref
resistive-type	hybrid polymer POM/Ppy	11−98% RH	1.9 s/1.1 s	this work
resistive-type	hybrid polymer PPy/ZnO	11−95% RH	180 s/60 s	18
impedance-type	hybrid polymer PPy/quaternized	11−95% RH	4 s/25 s	30
impedance-type	hybrid polymer PPy/graphene	12−90% RH	15 s/20 s	20
capacitance-type	PPy	25−85% RH	not applicable	14

response was measured at 80 °C, as demonstrated in Figure S11a in the Supporting Information. Figure S11b in the Supporting Information shows the dynamic characteristics at 98% RH for four cycles with a nearly invariable sensitivity, indicating the durability of the sensor operating at an elevated temperature. As shown above, the POM/Ppy humidity sensors exhibit good sensing properties, such as ultrafast response time, good stability, and good linearity. The humidity sensing properties of the polypyrrole and/or its composites with other inorganic materials found in the literature are summarized in Table 1.

CONCLUSION

In summary, a facile and green method was developed for the design and synthesis of POM/Ppy films and the fabrication of POM/Ppy nanocomposite-based resistive humidity sensors. The humidity sensing test results demonstrate that the as-prepared POM/Ppy nanocomposites exhibit excellent humidity sensing performance and elevated temperatures in comparison with those of other hybrid polymers of polypyrrole. The optimized POM/Ppy sample showed record rapid response/recovery times (1.9 s/1.1 s at 98% RH level, respectively), a sensing range of 11−98% RH, excellent durability, and repeatability with little hysteresis, which are superior to commercial thermosetting polyester (5 s, 20−80% RH, the data from Sensirion). By taking full advantage of the high hygroscopicity and water stability of the POMs and the hydrophobicity from the polypyrrole conducting polymer, the POM/Ppy-based humidity sensor exhibits both high sensitivity and a fast response time. Thus, we strongly believe that the POM/Ppy nanocomposite can act as a promising candidate in the future to develop ultrafast, low-priced, and highly sensitive humidity sensors.

ASSOCIATED CONTENT

Supporting Information

The Supporting Information is available free of charge on the ACS Publications website at DOI: 10.1021/acsanm.7b00072.

Preparation method of the reference material, table of thicknesses, response and recovery data, typical response curves, and dynamic responsive curves (PDF)

AUTHOR INFORMATION

Corresponding Authors

*E-mail: chengc@sustc.edu.cn.

*E-mail: zktang@umac.mo.

ORCID

Jun Miao: 0000-0002-9429-4681

Qingyin Wu: 0000-0002-3026-1186

Chun Cheng: 0000-0001-5976-3457

Notes

The authors declare no competing financial interest.

ACKNOWLEDGMENTS

This work was supported by Start-up Research Grant funding from University of Macau (Grant SRG2016-00002-FST), the Research and Development Grant for Chair Professor funding from University of Macau (Grant CPG2016-00026-FST), National Natural Science Foundation of China (Grants 51776094 and 51406075), Guangdong Natural Science Funds for Distinguished Young Scholars (Grant 2015A030306044), Guangdong−Hong Kong joint innovation project (Grant 2016A050503012), Training Program for Outstanding Young Teachers at Higher Education Institutions of Guangdong Province (Grant YQ2015151), National Key Research and Development Project funding from the Ministry of Science and Technology of China (Grants 2016YFA0202400, 2016YFA0202404, and 2016YFB0901600), Shenzhen Peacock Team Plan (Grant KQTD2015033110182370), and the Zhejiang Provincial Natural Science Foundation of China (Grant LY18B010001).

REFERENCES

(1) Yáñez-González, Á.; Ruiz-Trejo, E.; van Wachem, B.; Skinner, S.; Beyrau, F.; Heyes, A. Development of an optical thermal history coating sensor based on the oxidation of a divalent rare earth ion phosphor. *Meas. Sci. Technol.* **2016**, *27* (11), 115103.

(2) Raj, E. S.; Pratt, K. F. E.; Skinner, S. J.; Parkin, I. P.; Kilner, J. A. High Conductivity La2-xSrxCu1-y(Mg, Al)yO4 Solid State Metal Oxide Gas Sensors with the K2NiF4 Structure. *Chem. Mater.* **2006**, *18* (14), 3351−3355.

(3) Traversa, E. Ceramic sensors for humidity detection: the state-of-the-art and future developments. *Sens. Actuators, B* **1995**, *23* (2), 135−156.

(4) Adhikari, B.; Majumdar, S. Polymers in sensor applications. *Prog. Polym. Sci.* **2004**, *29* (7), 699−766.

(5) Chen, Z.; Lu, C. Humidity Sensors: A Review of Materials and Mechanisms. *Sens. Lett.* **2005**, *3* (4), 274−295.

(6) Packirisamy, M.; Stiharu, I.; Li, X.; Rinaldi, G. A polyimide based resistive humidity sensor. *Sens. Rev.* **2005**, *25* (4), 271−276.

(7) Farahani, H.; Wagiran, R.; Hamidon, M. Humidity Sensors Principle, Mechanism, and Fabrication Technologies: A Comprehensive Review. *Sensors* **2014**, *14* (5), 7881.

(8) Cai, J.; Huang, J.; Ge, M.; Iocozzia, J.; Lin, Z.; Zhang, K.-Q.; Lai, Y. Immobilization of Pt Nanoparticles via Rapid and Reusable Electropolymerization of Dopamine on TiO2 Nanotube Arrays for Reversible SERS Substrates and Nonenzymatic Glucose Sensors. *Small* **2017**, *13* (19), 1604240.

(9) Cheng, C.; Geng, H.; Yi, Y.; Shuai, Z. Super-exchange-induced high performance charge transport in donor-acceptor copolymers. *J. Mater. Chem. C* **2017**, *5* (13), 3247−3253.

(10) Gao, X.; Geng, H.; Peng, Q.; Ren, J.; Yi, Y.; Wang, D.; Shuai, Z. Nonadiabatic Molecular Dynamics Modeling of the Intrachain Charge Transport in Conjugated Diketopyrrolo-pyrrole Polymers. *J. Phys. Chem. C* **2014**, *118* (13), 6631−6640.

(11) Umeyama, T.; Miyata, T.; Jakowetz, A. C.; Shibata, S.; Kurotobi, K.; Higashino, T.; Koganezawa, T.; Tsujimoto, M.; Gelinas, S.; Matsuda, W.; Seki, S.; Friend, R. H.; Imahori, H. Regioisomer effects of [70]fullerene mono-adduct acceptors in bulk heterojunction polymer solar cells. *Chemical Science* **2017**, *8* (1), 181−188.

(12) Smith, M. J.; Malak, S. T.; Jung, J.; Yoon, Y. J.; Lin, C. H.; Kim, S.; Lee, K. M.; Ma, R.; White, T. J.; Bunning, T. J.; Lin, Z.; Tsukruk, V. V. Robust, Uniform, and Highly Emissive Quantum Dot−Polymer Films and Patterns Using Thiol−Ene Chemistry. *ACS Appl. Mater. Interfaces* **2017**, *9* (20), 17435−17448.
(13) Kukla, A. L.; Pavluchenko, A. S.; Shirshov, Y. M.; Konoshchuk, N. V.; Posudievsky, O. Y. Application of sensor arrays based on thin films of conducting polymers for chemical recognition of volatile organic solvents. *Sens. Actuators, B* **2009**, *135* (2), 541−551.
(14) Yang, M.-Z.; Dai, C.-L.; Lu, D.-H. Polypyrrole Porous Micro Humidity Sensor Integrated with a Ring Oscillator Circuit on Chip. *Sensors* **2010**, *10* (11), 10095.
(15) Nohria, R.; Su, Y.; Khillan, R. K.; Dikshit, R.; Lvov, Y.; Varahramyan, K. Development of Humidity Sensors using Layer-by-Layer nanoAssembly of Polypyrrole. *MRS Online Proc. Libr.* **2005**, *872*, 872.
(16) Anwar, N.; Vagin, M.; Laffir, F.; Armstrong, G.; Dickinson, C.; McCormac, T. Transition metal ion-substituted polyoxometalates entrapped in polypyrrole as an electrochemical sensor for hydrogen peroxide. *Analyst* **2012**, *137* (3), 624−630.
(17) Sun, C.; Wang, D.; Zhang, M.; Ni, Y.; Shen, X.; Song, Y.; Geng, Z.; Xu, W.; Liu, F.; Mao, C. Novel l-lactic acid biosensors based on conducting polypyrrole-block copolymer nanoparticles. *Analyst* **2015**, *140* (3), 797−802.
(18) Najjar, R.; Nematdoust, S. A resistive-type humidity sensor based on polypyrrole and ZnO nanoparticles: hybrid polymers vis-a-vis nanocomposites. *RSC Adv.* **2016**, *6* (113), 112129−112139.
(19) Yang, M.; Hong, S. B.; Yoon, J. H.; Kim, D. S.; Jeong, S. W.; Yoo, D. E.; Lee, T. J.; Lee, K. G.; Lee, S. J.; Choi, B. G. Fabrication of Flexible, Redoxable, and Conductive Nanopillar Arrays with Enhanced Electrochemical Performance. *ACS Appl. Mater. Interfaces* **2016**, *8* (34), 22220−22226.
(20) Lin, W.-D.; Chang, H.-M.; Wu, R.-J. Applied novel sensing material graphene/polypyrrole for humidity sensor. *Sens. Actuators, B* **2013**, *181*, 326−331.
(21) Kano, S.; Kim, K.; Fujii, M. Fast-Response and Flexible Nanocrystal-Based Humidity Sensor for Monitoring Human Respiration and Water Evaporation on Skin. *ACS Sensors* **2017**, *2* (6), 828−833.
(22) Yan, H.; Zhang, L.; Yu, P.; Mao, L. Sensitive and Fast Humidity Sensor Based on A Redox Conducting Supramolecular Ionic Material for Respiration Monitoring. *Anal. Chem.* **2017**, *89* (1), 996−1001.
(23) Kuang, Q.; Lao, C.; Wang, Z. L.; Xie, Z.; Zheng, L. High-Sensitivity Humidity Sensor Based on a Single SnO2 Nanowire. *J. Am. Chem. Soc.* **2007**, *129* (19), 6070−6071.
(24) Yassine, O.; Shekhah, O.; Assen, A. H.; Belmabkhout, Y.; Salama, K. N.; Eddaoudi, M. H2S Sensors: Fumarate-Based fcu-MOF Thin Film Grown on a Capacitive Interdigitated Electrode. *Angew. Chem., Int. Ed.* **2016**, *55* (51), 15879−15883.
(25) Deng, J.; Ma, J.; Mei, L.; Tang, Y.; Chen, Y.; Lv, T.; Xu, Z.; Wang, T. Porous [small alpha]-Fe2O3 nanosphere-based H2S sensor with fast response, high selectivity and enhanced sensitivity. *J. Mater. Chem. A* **2013**, *1* (40), 12400−12403.
(26) Li, H.; Liu, B.; Cai, D.; Wang, Y.; Liu, Y.; Mei, L.; Wang, L.; Wang, D.; Li, Q.; Wang, T. High-temperature humidity sensors based on WO3-SnO2 composite hollow nanospheres. *J. Mater. Chem. A* **2014**, *2* (19), 6854−6862.
(27) Wang, Y.; Liu, B.; Xiao, S.; Li, H.; Wang, L.; Cai, D.; Wang, D.; Liu, Y.; Li, Q.; Wang, T. High performance and negative temperature coefficient of low temperature hydrogen gas sensors using palladium decorated tungsten oxide. *J. Mater. Chem. A* **2015**, *3* (3), 1317−1324.
(28) Cai, D.; Liu, B.; Wang, D.; Wang, L.; Liu, Y.; Qu, B.; Duan, X.; Li, Q.; Wang, T. Rational synthesis of metal-organic framework composites, hollow structures and their derived porous mixed metal oxide hollow structures. *J. Mater. Chem. A* **2016**, *4* (1), 183−192.
(29) Burman, D.; Ghosh, R.; Santra, S.; Guha, P. K. Highly proton conducting MoS2/graphene oxide nanocomposite based chemo-resistive humidity sensor. *RSC Adv.* **2016**, *6* (62), 57424−57433.
(30) Li, X.-Z.; Liu, S.-R.; Guo, Y. Polyaniline-intercalated layered double hydroxides: synthesis and properties for humidity sensing. *RSC Adv.* **2016**, *6* (68), 63099−63106.
(31) Herrmann, S.; Ritchie, C.; Streb, C. Polyoxometalate - conductive polymer composites for energy conversion, energy storage and nanostructured sensors. *Dalton Transactions* **2015**, *44* (16), 7092−7104.
(32) Ji, Y.; Huang, L.; Hu, J.; Streb, C.; Song, Y.-F. Polyoxometalate-functionalized nanocarbon materials for energy conversion, energy storage and sensor systems. *Energy Environ. Sci.* **2015**, *8* (3), 776−789.
(33) Ammam, M. Polyoxometalates: formation, structures, principal properties, main deposition methods and application in sensing. *J. Mater. Chem. A* **2013**, *1* (21), 6291−6312.
(34) Sumliner, J. M.; Lv, H.; Fielden, J.; Geletii, Y. V.; Hill, C. L. Polyoxometalate Multi-Electron-Transfer Catalytic Systems for Water Splitting. *Eur. J. Inorg. Chem.* **2014**, *2014* (4), 635−644.
(35) Lv, H.; Geletii, Y. V.; Zhao, C.; Vickers, J. W.; Zhu, G.; Luo, Z.; Song, J.; Lian, T.; Musaev, D. G.; Hill, C. L. Polyoxometalate water oxidation catalysts and the production of green fuel. *Chem. Soc. Rev.* **2012**, *41* (22), 7572−7589.
(36) Li, J.-S.; Wang, Y.; Liu, C.-H.; Li, S.-L.; Wang, Y.-G.; Dong, L.-Z.; Dai, Z.-H.; Li, Y.-F.; Lan, Y.-Q. Coupled molybdenum carbide and reduced graphene oxide electrocatalysts for efficient hydrogen evolution. *Nat. Commun.* **2016**, *7*, 11204.
(37) Seino, S.; Kawahara, R.; Ogasawara, Y.; Mizuno, N.; Uchida, S. Reduction-Induced Highly Selective Uptake of Cesium Ions by an Ionic Crystal Based on Silicododecamolybdate. *Angew. Chem., Int. Ed.* **2016**, *55* (12), 3987−3991.
(38) Pope, M. T.; Müller, A. Polyoxometalate Chemistry: An Old Field with New Dimensions in Several Disciplines. *Angew. Chem., Int. Ed. Engl.* **1991**, *30* (1), 34−48.
(39) Long, D.-L.; Burkholder, E.; Cronin, L. Polyoxometalate clusters, nanostructures and materials: From self assembly to designer materials and devices. *Chem. Soc. Rev.* **2007**, *36* (1), 105−121.
(40) Kawahara, R.; Uchida, S.; Mizuno, N. Redox-Induced Reversible Uptake−Release of Cations in Porous Ionic Crystals Based on Polyoxometalate: Cooperative Migration of Electrons with Alkali Metal Ions. *Chem. Mater.* **2015**, *27* (6), 2092−2099.
(41) Li, S.; Zhang, F.; Peng, Q.; Chen, X.; Wang, R.; Wang, Z.; Ma, F.; Zhao, Q.; Wei, M. A sandwich-type POM containing mixed cations: synthesis, thermal performance and proton-conducting properties. *J. Coord. Chem.* **2016**, *69* (3), 425−432.
(42) Peng, Q.; Li, S.; Wang, R.; Liu, S.; Xie, L.; Zhai, J.; Zhang, J.; Zhao, Q.; Chen, X. Lanthanide derivatives of Ta/W mixed-addendum POMs as proton-conducting materials. *Dalton Transactions* **2017**, *46* (13), 4157−4160.
(43) Tsuboi, M.; Hibino, M.; Mizuno, N.; Uchida, S. Crystalline polyoxometalate (POM)−polyethylene glycol (PEG) composites aimed as non-humidified intermediate-temperature proton conductors. *J. Solid State Chem.* **2016**, *234*, 9−14.
(44) Li, Y. Effect of anion concentration on the kinetics of electrochemical polymerization of pyrrole. *J. Electroanal. Chem.* **1997**, *433* (1), 181−186.
(45) Singh, A.; Salmi, Z.; Joshi, N.; Jha, P.; Decorse, P.; Lecoq, H.; Lau-Truong, S.; Jouini, M.; Aswal, D. K.; Chehimi, M. M. Electrochemical investigation of free-standing polypyrrole-silver nanocomposite films: a substrate free electrode material for supercapacitors. *RSC Adv.* **2013**, *3* (46), 24567−24575.
(46) Li, M.; Wei, Z.; Jiang, L. Polypyrrole nanofiber arrays synthesized by a biphasic electrochemical strategy. *J. Mater. Chem.* **2008**, *18* (19), 2276−2280.
(47) Cuentas-Gallegos, A. K.; Frausto, C.; Ortiz-Frade, L. A.; Orozco, G. Raman spectra of hybrid materials based on carbon nanotubes and Cs3PMo12O40. *Vib. Spectrosc.* **2011**, *57* (1), 49−54.
(48) Li, Y.; Yang, J. Effect of electrolyte concentration on the properties of the electropolymerized polypyrrole films. *J. Appl. Polym. Sci.* **1997**, *65* (13), 2739−2744.
(49) Uchida, S.; Inumaru, K.; Misono, M. States and Dynamic Behavior of Protons and Water Molecules in H3PW12O40

DOI: 10.1021/acsanm.7b00072
ACS Appl. Nano Mater. 2018, 1, 564−571

Pseudoliquid Phase Analyzed by Solid-State MAS NMR. *J. Phys. Chem. B* **2000**, *104* (34), 8108−8115.
(50) Zhang, X.-W.; Pan, Y.; Zheng, Q.; Yi, X.-S. Time dependence of piezoresistance for the conductor-filled polymer composites. *J. Polym. Sci., Part B: Polym. Phys.* **2000**, *38* (21), 2739−2749.
(51) Geng, W.; Wang, R.; Li, X.; Zou, Y.; Zhang, T.; Tu, J.; He, Y.; Li, N. Humidity sensitive property of Li-doped mesoporous silica SBA-15. *Sens. Actuators, B* **2007**, *127* (2), 323−329.
(52) Nakamura, O.; Kodama, T.; Ogino, I.; Miyake, Y. HIGH-CONDUCTIVITY SOLID PROTON CONDUCTORS: DODECAMOLYBDOPHOSPHORIC ACID AND DODECATUNGSTOPHOSPHORIC ACID CRYSTALS. *Chem. Lett.* **1979**, *8* (1), 17−18.
(53) Liu, Y.; Liu, S.; Lai, X.; Miao, J.; He, D.; Li, N.; Luo, F.; Shi, Z.; Liu, S. Polyoxometalate-Modified Sponge-Like Graphene Oxide Monolith with High Proton-Conducting Performance. *Adv. Funct. Mater.* **2015**, *25* (28), 4480−4485.
(54) Lai, X.; Liu, Y.; Yang, G.; Liu, S.; Shi, Z.; Lu, Y.; Luo, F.; Liu, S. Controllable proton-conducting pathways via situating polyoxometalates in targeting pores of a metal-organic framework. *J. Mater. Chem. A* **2017**, *5* (20), 9611−9617.
(55) Liu, Y.; Yang, X.; Miao, J.; Tang, Q.; Liu, S.; Shi, Z.; Liu, S. Polyoxometalate-functionalized metal-organic frameworks with improved water retention and uniform proton-conducting pathways in three orthogonal directions. *Chem. Commun.* **2014**, *50* (70), 10023−10026.
(56) Miao, J.; Liu, Y.; Tang, Q.; He, D.; Yang, G.; Shi, Z.; Liu, S.; Wu, Q. Proton conductive watery channels constructed by Anderson polyanions and lanthanide coordination cations. *Dalton Transactions* **2014**, *43* (39), 14749−14755.
(57) Li, Y.; Qian, R.; Imaeda, K.; Inokuchi, H. Behavior of the High Temperature Conductivity of Polypyrrole Nitrate Films. *Polym. J.* **1994**, *26* (5), 535−538.

DOI: 10.1021/acsanm.7b00072
ACS Appl. Nano Mater. 2018, 1, 564−571